

ORIGINAL RESEARCH ARTICLE

Effect of fused deposition modeling process parameter in influence of mechanical property of acrylonitrile butadiene styrene polymer

Raja Subramani^{1,*}, Arun Kumar Kalidass², Mohan Dass Muneeswaran³, Balaji Gantala Lakshmipathi⁴

¹ Research & Development, Mr.R Business Corporation, Karur 639002, India

² Department of Mechanical Engineering, Karpagam College of Engineering, Coimbatore 641032, India

³ Department of Mechanical Engineering, Coimbatore Institute of Engineering and Technology, Thondamuthur 641109, India

⁴ Department of Research and Innovation, Saveetha School of Engineering, Saveetha Institute of Medical and Technical Sciences, Chennai 602105, India

* Corresponding author: Raja Subramani, engineerraja@yahoo.com

ABSTRACT

The objective of this study is to investigate how the mechanical properties of components produced using acrylonitrile butadiene styrene (ABS) on a Creality Ender-3 3D printer are affected by various fused deposition modeling (FDM) printing parameters. The impact of various factors, including infill density, printing speed, platform temperature, extruder temperature, and so on, was assessed in terms of their influence on the ultimate tensile strength, yield strength, and elastic modulus of the manufactured components. The impact of each parameter was assessed using a Multi-criteria decision-making (MCDM) methodology. Finally, the second set of parameters, including a 35% infill thickness, 0.25 mm layer level, 40 mm/s printing speed, 75 °C platform temperature, 210 °C extruder temperature, and 75 mm/s travel speed, was discovered to be the most suitable for ABS filament used to make impellers.

Keywords: fused deposition modeling; thermoplastic polymer; 3D printing; mechanical property; process parameter analysis

ARTICLE INFO

Received: 8 December 2023
Accepted: 21 December 2023
Available online: 18 January 2024

COPYRIGHT

Copyright © 2024 by author(s).
Applied Chemical Engineering is published by
EnPress Publisher, LLC. This work is licensed
under the Creative Commons Attribution-
NonCommercial 4.0 International License
(CC BY-NC 4.0).
<https://creativecommons.org/licenses/by-nc/4.0/>

1. Introduction

Over the recent years, additive manufacturing (AM) has become a collection of potent technologies capable of facilitating innovative approaches, using a wide variety of materials, such as metals and plastics. These technologies are employed for creating prototypes and final products^[1-7]. Fused Deposition Modeling (FDM) has gained growing interest because of its inherent simplicity, adaptability, and affordability. FDM involves a manufacturing method wherein, under controlled circumstances, a heated thermoplastic filament is extruded onto a platform along the xy plane and it can show in **Figure 1**. The construction of the 3D component involves reducing the platform in the z-direction to produce successive layers stacked on top of each other during printing. Acrylonitrile butadiene styrene (ABS) stands out as a widely utilized material in FDM due to its widespread availability and its ability to produce components of superior quality, tenacity, and longevity. To meet the ultimate details of the product, it is essential to anticipate the mechanical characteristics of the produced components and materials. This involves comprehending the impact of these properties' FDM printing parameters. Understanding the correlation

between the mechanical and FDM printing parameters characteristics is crucial for creating dependable 3D printed functional components. While factors like machine settings, CAD models, environmental conditions and properties of thermoplastic filaments contribute to the end result, the primary input variables with the most notable influence on the mechanical qualities of the produced parts are the FDM processing parameters. Despite a growing body of research utilizing experimental procedures and experiment design like the Single factorial designs, Taguchi method, or ANOVA to investigate how parameters for the FDM process impact the quality of produced parts, the complexity arises from the multitude of parameters, levels, combined effects, and result variability^[8–20]. This complexity makes discussing the mechanical characteristics of FDM components challenging task. This research aims to make a significant contribution to the discussion on the mechanical characteristics of ABS components manufactured through FDM. It concentrates on exploring the impact of various factors using MCDM method, including infill density, printing speed, platform temperature, extruder temperature, and so on.

2. Materials and methods

Fused deposition modeling relies layer by layer, in accordance with the 3D model, during the hot melt extrusion process information until a complete object is formed. In this process, a filament feedstock, typically with a diameter of either 3.00 mm or 1.75 mm, is fed into a printer using a drive gear mechanism that revolves. One of the drive mechanisms is connected to a stepper motor, providing the energy to move the filament that passes via the system. A notched or toothed surface on both drive gears may be used to provide enough friction so that the drive gear can grip the filament and feed it to the liquefier without slipping^[21–26]. The solid portion of the filament then functions as a piston to force the melted material through the print nozzle when the filament is melted in the heated liquefier and it can show in **Figure 1**. The specimens of ASTM D638 Type V were produced using Creality Ender-3 3D printer and ABS filament from the same brand. Creo was used to design the 3D models, which were afterwards exported as files in Standard Triangle Language (STL). These STL files were processed in Flashforge 5.0 slicing software to generate the corresponding G.code file^[27–31].

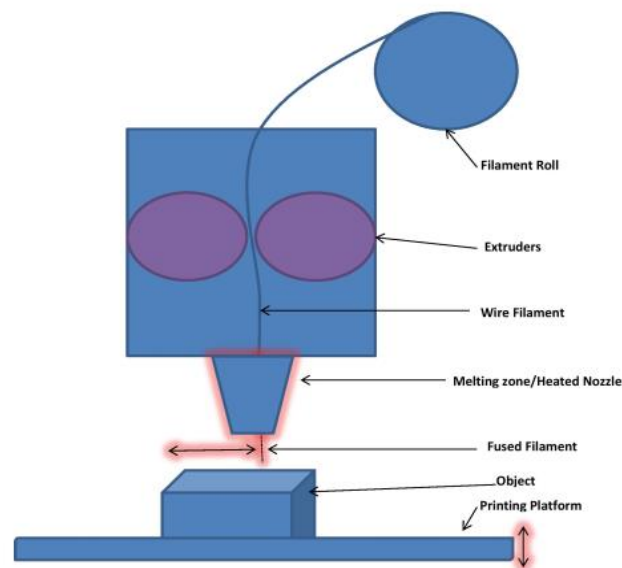


Figure 1. Fused Deposited Modelling (FDM) printing process.

2.1. Assumptions of the research

Discovering the optimal printing parameters for ABS, considering data on ultimate tensile strength, Young’s modulus, Ultimate flexural strength and surface defects, is essential for the impeller application. To achieve this, the following assumption is taken into account^[32–39].

- This analysis takes into account multiple process parameters that influence the mechanical characteristics of the final product.
- The evaluation framework is formulated based on the outcomes derived from available data. Tensile test UTS results constitute Criteria 1 (C1), young’s modulus results make up Criteria 2 (C2), Criteria 3 (C3) is ultimate flexural strength and FESEM test results define Criteria 4 (C4). Specifically, the alternatives A1, A2, A3, A4, and A5 are explicitly mentioned instead of using the labels Sample 1, Sample 2, Sample 3, Sample 4, and Sample 5.
- Similarly, the triangular membership function is derived from the FAHP technique, incorporating a set of five parameters according to the TOPSIS strategy in semantics. Consequently, the assessment of criteria is conducted with a focus on mechanical properties, ultimately determining the optimal parameter set for impeller manufacturing among the alternatives.
- During this assessment, the Creality Ender-3 serves as the 3D printer, and the slicing software employed is Flash Forge 5.0. Consequently, outcomes may vary when utilizing alternative technologies
- The printing parameter for ABS in this study has been applied within a range spanning from the minimum to the maximum values, as reported in earlier literature.
- During this assessment, the Infill printing parameter is set to the standard line. Therefore, it has the flexibility to transition when employing alternative infill designs such as hexagonal, triangle, and so forth.
- Every mentioned sample corresponds to a specific set of parameters (a cluster of process parameters, as illustrated in **Table 1**).

Table 1. Process parameter taken for ABS.

Process parameter	Sample 1	Sample 2	Sample 3	Sample 4	Sample 5
Infill pattern	Line				
Infill density (%)	30	35	40	45	50
Layer height (mm)	0.30	0.25	0.20	0.15	0.10
Print speed (mm/s)	30	40	50	60	70
Platform temperature (°C)	70	75	80	85	90
Extruder temperature (°C)	200	210	220	230	240
Travel speed (mm/s)	70	75	80	85	90

2.2. Tensile test

Tensile experiments were conducted using an INSTRON 5566J975 universal testing machine at a strain rate of 1 mm/min. The tensile test parameters (ultimate tensile strength, yield strength, and Young’s modulus) were assessed following ASTM 638 Type V guidelines and derived from the stress-strain relationship. The samples were produced and subjected to tensile testing in a randomized sequence.

2.3. Multi-criteria decision-making (MCDM)

MCDM involves selecting the best choice among a number of options. Earlier scholars have employed this approach in intricate decision-making scenarios across various domains. The MCDM methodology has been referenced in previous academic works under various labels, including Multi-Criteria Decision Analysis (MCDA). Andrearczyk et al.^[18] conducted a comprehensive review, investigating the widespread application of the MCDM method in both qualitative and quantitative research according to previous literature. The hierarchical structure of the MCDM method is illustrated, with further elaboration provided in section 3. Various MCDM tools, such as BWM (Best Worst Method), AHP (Analytical Hierarchy Process), ANP (Analytical Network Process), COPRAS (Complex PROportional Assessment), TOPSIS (Technique for Order of Preference by Similarity to Ideal Solution), FAHP (Fuzzy Analytical Hierarchy Process) and PROMETHEE

(Preference Ranking Organization Method for Enrichment of Evaluations), are utilized. The decision-making process involves creating a pairwise matrix based on the decision maker's opinions, converting it into numerical values ranging from 0 to 9 (depending on the MCDM tool/technique)^[40-57]. Subsequently, the pairwise matrix undergoes evaluation through fundamental steps like criteria weight determination, consistency ratio assessment, and random index calculation^[58-63]. Ultimately, alternatives are ranked using the decision matrix and priority values, and the most suitable alternative is selected for the decision maker based on the ranking.

2.4. Field emission scanning electron microscopy (FESEM)

FESEM was used to examine the external and fracture surfaces of ABS specimens. The FESEM images were captured utilizing a field emission type microscope with an operating voltage of 20.0 kV, employing a mode of secondary electron emission. The samples were attached to the FESEM sample holder using conductive adhesive (gold sputter coating), and prior to the coating process on a sputtering system, the sample surface was cleaned using an air flux (QuorumQ150TES).

3. Results

3.1. Tensile observation

The Tinius Olsen H10KL machine conducted tensile testing on three samples for each set of parameters, resulting in a total of 15 samples across five parameter sets. **Tables 2** and **3** show the values for UTS (ultimate tensile strength) and Young's modulus respectively. Trials A, B, and C were employed for testing each parameter set, and the average results were computed for assessing criteria using linguistic terms for UTS and Young's modulus.

Table 2 presents the ultimate tensile strength values for each specimen in trials I, II, and III. The linguistic term has been assigned according to the average value, as detailed in **Table 4**. It is observed that Sample 2 exhibits the highest average ultimate tensile strength, whereas Sample 5 has the lowest. Ratings of Very High (VH) and Very Low (VL) on the linguistic term scale were assigned to Samples 2 and 5, respectively.

Table 2. Tensile test UTS observation.

TRIAL	Ultimate Tensile Strength (MPa)				
	Sample-1	Sample-2	Sample-3	Sample-4	Sample-5
I	30.7	37.2	42.0	30.2	29.4
II	29.4	40.6	33.1	36.2	28.4
III	39.8	38.9	30.6	40.1	19.4
Average	33.3	38.9	35.2	35.5	25.7
Importance	L	VH	A	H	VL

The Young's modulus values for specimens in experiments A, B, and C are presented in **Table 3**. **Table 4** assigns linguistic terms based on the average values. Notably, Sample 4 exhibits the lowest average Young's modulus, whereas Sample 3 demonstrates the highest. Consequently, Sample 3 is categorized as Very High (VH) on the linguistic term scale, while Sample 4 is classified as Very Low (VL).

Table 3. Tensile test for Young's Modulus observation.

TRIAL	Young's Modulus (MPa)				
	Sample-1	Sample-2	Sample-3	Sample-4	Sample-5
A	512	584	612	563	548
B	529	562	606	495	586

Table 3. (Continued).

TRIAL	Young's Modulus (MPa)				
	Sample-1	Sample-2	Sample-3	Sample-4	Sample-5
C	596	523	625	523	592
Average	545.6	556.3	614.3	527	575.3
Importance	L	A	VH	VL	H

Table 4. Criteria evaluation by Fuzzy TOPSIS scale.

Common Criteria's and sorted different set of parameters (samples) based on importance from result obtained				TOPSIS scale ^[42]		
UTS	Youngs modulus	UFS	FESEM	Linguistics terms	Linguistics scales	Triangular membership function-based fuzzy values
5	4	5	4	Very Low (VL)	1	1,1,3
1	1	3	1	Low (L)	2	1,3,5
3	2	4	2	Average (A)	3	3,5,7
4	5	1	3	High (H)	4	5,7,9
2	3	2	5	Very High (VH)	5	7,9,9

3.2. Three-point bending observation

Three-point bending experiments were employed to evaluate both the flexural strength and modulus of the composites, along with examining the failure surface morphology. This investigation aimed to comprehend the failure mechanism and deformation process of the composites. Across three trials (designated as A, B, and C), the flexural stress for each sample was computed using the three-point bending test. Criteria 3 were established to evaluate different samples by considering the average value derived from the flexural test observations and the outcomes of the flexural modulus.

The ultimate flexure strength values for each specimen in trials A, B, and C can be found in **Table 5**. Additionally, **Table 4** includes linguistic terms assigned based on the average values. It is noteworthy that Sample 2 exhibits the highest average Ultimate Flexure Strength, whereas Sample 5 has the lowest value. Consequently, Sample 2 is categorized as Very High (VH) on the linguistic term scale, while Sample 5 is labeled as Very Low (VL).

Table 5. Flexure test observation.

TRIAL	Ultimate Flexure Strength (MPa)				
	Sample-1	Sample-2	Sample-3	Sample-4	Sample-5
A	19.36	28.65	12.63	29.63	12.36
B	26.95	31.23	16.25	22.56	14.25
C	30.25	30.2	19.65	21.47	16.84
Average	25.52	30.02	16.17	24.55	14.48
Importance	H	VH	L	A	VL

3.3. Morphology analysis

Analyzed through FESEM examination were altered printing parameter samples, revealing microstructure defects. Subsequently, morphology analysis assessed criteria 4 on a linguistic scale (1–5) based on these findings. The ABS samples with a gold sputter coating during FESEM analysis, enhancing the conductivity of non-conductive materials. Based on the morphological analysis, Sample 5 exhibits a remarkably sleek upper surface with fewer and more robust linear pattern indentations. In contrast, Sample 4

displays a coarse surface and inadequate infill. As Sample 5 is currently assigned a Very High (VH) priority, Sample 4 is now designated with a Very Low (VL) priority. The morphology of the five distinct samples is illustrated in **Figure 2**.

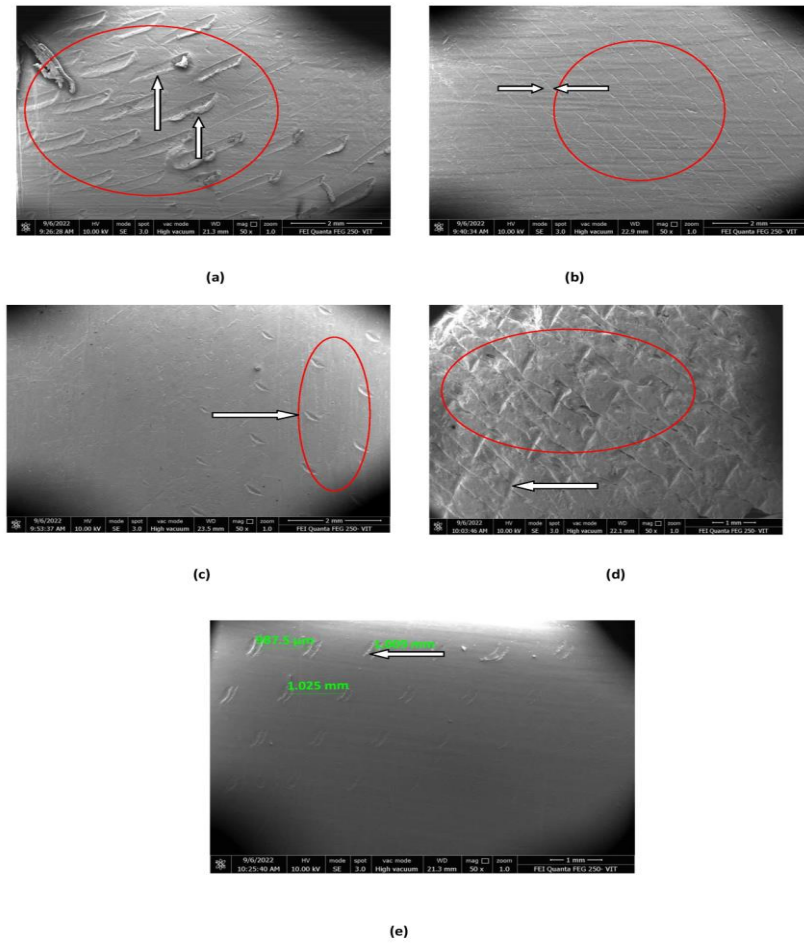


Figure 2. Morphology of printed samples (a) Sample 1; (b) Sample 2; (c) Sample 3; (d) Sample 4; (e) Sample 5.

3.4. Formatting of mathematical components

Using the gathered information, **Table 4** was generated. The triangular membership function converts linguistic expressions into linguistic scales and then translates linguistic scales into fuzzy values.

Tables 6 and **7** present an assessment matrix for an alternative, utilizing criteria outlined in **Table 4** and the triangular membership function, respectively (see **Table 4** for reference). As an example, consider Alternative 1 (Sample 1) in the first row and first column of **Table 6**, which demonstrates a high (H) importance concerning Criteria 1. This value is substituted by the triangular membership function values 5, 7, 9 in the corresponding position of **Table 7**. Subsequently, the maximum value in each column is divided by the individual values across all columns. **Table 8** represents the fuzzy positive ideal solution (A^*), calculated by selecting the maximum value from each column in the favorable criteria. In addition to morphology criteria, this study incorporates useful criteria to enhance mechanical properties. To determine the fuzzy negative ideal solution, the subsequent step involves minimizing each column's cost criterion (A^-).

Table 6. Evaluation matrix by Linguistic scale.

	C1	C2	C3	C4
A1	L	L	H	L
A2	VH	A	VH	A
A3	A	VH	L	H
A4	H	VL	A	VL
A5	VL	H	VL	VH

Table 7. Evaluation matrix with triangular membership function.

	C1			C2			C3			C4		
A1	1	3	5	1	3	5	5	7	9	1	3	5
A2	7	9	9	3	5	7	7	9	9	3	5	7
A3	3	5	7	7	9	9	1	3	5	5	7	9
A4	5	7	9	1	1	3	3	5	7	1	1	3
A5	1	1	3	5	7	9	1	1	3	7	9	9

Table 8. Estimate the fuzzy positive ideal solution (A*) and negative ideal solution (A-).

	C1			C2			C3			C4		
Normalized decision matrix												
A1	0.111111111	0.3333333	0.555555556	0.111111111	0.3333333	0.555556	0.555556	0.777778	1	0.2	0.333333	1
A2	0.777777778	1	1	0.333333333	0.555556	0.777778	0.777778	1	1	0.142857	0.2	0.333333
A3	0.333333333	0.555556	0.777777778	0.777777778	1	1	0.111111	0.333333	0.555556	0.111111	0.142857	0.2
A4	0.555555556	0.777778	1	0.111111111	0.111111	0.333333	0.333333	0.555556	0.777778	0.333333	1	1
A5	0.111111111	0.111111	0.333333333	0.555555556	0.777778	1	0.111111	0.111111	0.333333	0.111111	0.111111	0.142857

Table 9. Estimate the distance from each alternative FPIS (A*).

	C1	C2	C3	C4	di*
A1	0	0.6017807	0	0.601780705	1.203561
A2	1.283×10^{-7}	0.3849003	1.283×10^{-7}	0.384900265	0.769801
A3	0.384900265	1.283×10^{-7}	0.601780705	0.181443775	1.168125
A4	0.798661432	0.7481115	0.384900265	0.748111543	2.679785
A5	0.748111543	0	0.748111543	0	1.496223

Table 9 presents the distances of individual alternatives from the fuzzy positive ideal solution, whereas **Table 10** illustrates the distances of the fuzzy ideal solution from each alternative. The calculation of these distances can be performed using the provided Equation (1).

$$d(\dot{x}, \dot{y}) = sq\sqrt{\frac{1}{3} \times [(a1 - a2)^2 + (b1 - b2)^2 + (c1 - c2)^2]} \quad (1)$$

If a1 represents the A* value for each column, and a2 denotes the individual value within each column, the fuzzy positive ideal solution is defined by a1. A1 and A2 function as variables for the values in each column during the computation of the fuzzy negative ideal solution. The aggregate sums are presented in **Tables 9 and 10**. In the fuzzy positive ideal solution, the total values exhibit di* notation, while the total values exhibit di- in the fuzzy negative ideal solution.

Table 10. Estimate the distance from every other FNIS (A-).

	C1	C2	C3	C4	di-
A1	0.181443866	0	0.601780814	0.181443866	0.964669
A2	0	0.3849004	0.748111653	0.384900372	1.517912
A3	0.384900372	0.7481117	0.181443866	0.601780814	1.916237
A4	0.601780814	2.128×10^{-7}	0	0	0.601781
A5	2.12762×10^{-7}	0.6017808	2.12762×10^{-7}	0.748111653	1.349893

4. Discussion

Based on previous research findings^[64–67], UTS plays a significant role in determining tensile outcomes. Consequently, sample 2 exhibits the highest strength at 35.7 MPa, securing the top position, followed by sample 1 at 34.6 MPa (second), sample 3 at 32.1 MPa (third), sample 4 at 27.9 MPa (fourth), and sample 5 at 19.8 MPa (fifth). This implies that the TOPSIS Linguistics scale assigns a high importance of 5 points to sample 2 with high strength and a low importance of 1 point to sample 5 with low strength.

Similarly, as per earlier research^[68–71], Young's Modulus significantly influences tensile outcomes. Consequently, sample 3 demonstrates the highest strength at 591 MPa, securing the top position, followed by sample 1 at 571 MPa (second), sample 2 at 556 MPa (third), sample 5 at 502 MPa (fourth), and sample 4 at 496 MPa (fifth). Accordingly, the TOPSIS Linguistics scale assigns a high importance of 5 points to high-strength samples like sample 3 and a low importance of 1 point to low-strength samples such as sample 4, indicating their relative significance.

As per previous research papers^[72], the Ultimate Flexure Strength holds significant importance in determining flexural outcomes. Notably, sample 2 exhibits the highest strength at 26.628 MPa, followed by sample 1 at 21.523 MPa, sample 3 at 19.572 MPa, sample 4 at 18.116 MPa, and sample 5 at 12.968 MPa. Consequently, the TOPSIS Linguistics scale assigns a high importance of 5 points to the high-strength sample 2 and a very low importance of 1 point to the low-strength sample 5.

In the context of morphological findings, this study focuses on surface roughness and defects. Based on the obtained information, sample 5 exhibits a smooth surface finish with fewer defects compared to sample 3. Sample 2, on the other hand, has a slightly smoother surface finish and fewer lines than sample 4. In contrast, sample 1 has a rougher surface than the other specimens and is ranked fifth due to numerous surface flaws, including pores, gaps, and other imperfections. Consequently, the TOPSIS Linguistics scale assigns a high importance of 5 points to the high-strength sample 5 and a very low importance of 1 point to the low-strength sample 1.

The presented decision matrix was formulated through a thorough analysis of both criteria and alternatives. **Table 11** shows the ranking of the alternatives, determined using the coefficient of closeness as per the applied calculation Equation (2).

$$CC_i = \frac{di^-}{di^- + di^*} \quad (2)$$

Table 11. Ranking based on Cci.

	Co-efficient of closeness (Cci)	Rank
A1	0.444910626	IV
A2	0.663506425	I
A3	0.621274989	II
A4	0.183382282	V
A5	0.474293002	III

According to the observation, Sample 2 displayed the highest coefficient of closeness value among various samples. In comparison with other samples, the parameters of Sample 2 exhibit the superior mechanical properties for producing impellers. The combination of parameters, including 35% infill thickness, 0.25 mm layer height, 40 mm/s printing speed, 75 °C platform temperature, 210 °C extruder temperature, and 75 mm/s travel speed, was identified as the optimal configuration for using ABS in impeller manufacturing.

5. Conclusion

The recent rise in the adoption of additive manufacturing (AM) technologies is attributed to their numerous advantages over traditional manufacturing methods. AM offers benefits such as enhanced design flexibility, reduced cycle times, customization of products, and progress in green technology. Although there is a growing focus on using AM for end-use components, the planning process for AM remains challenging due to its complexity, the evolving landscape of AM technologies, and the diversity among AM product and service providers. Consequently, to advance AM management, it is crucial to engage in long-term and strategically planned effective AM planning.

This research employs integrative MCDM to analyze the selection of process parameters for the material extrusion of ABS impellers. The Fuzzy TOPSIS is utilized to assess the weights of criteria influencing the selection of parameters for the material extrusion process.

Several assumptions underlie the research objective, with a primary assumption being that a set (cluster) of process parameters significantly impacts the mechanical properties of products produced through material extrusion. The study examines five sets of printing parameters as alternatives and considers mechanical properties, including UTS, Young's modulus, ultimate flexural strength, and morphology, as criteria for producing tensile and flexural specimens using selected ABS filament.

Following the experimental findings, an evaluation is conducted without a decision maker, and a Pairwise matrix is created using linguistic terms. The matrix is then solved using triangular membership functions.

Ultimately, based on the ranking derived from the Fuzzy TOPSIS approach, sample 2 is identified as the suitable set of printing parameters.

Future research directions include evaluating experimental data using MCDM methods as alternatives to statistical tools employed by previous researchers. Additionally, exploring composite polymer printing parameters for rotating component applications and investigating the combined effect of process parameters on mechanical properties represent potential research avenues.

Author contributions

Conceptualization, RS; methodology, RS; validation, RS, and BGL; formal analysis, RS and MDM; investigation, RS; resources, RS; data duration, RS; writing—original draft preparation, RS and MDM; writing—review and editing, RS and AKK; supervision, RS and MDM. All authors have read and agreed to the published version of the manuscript.

Funding

The authors claimed that they were not compensated for writing this research and writing.

Acknowledgments

This research project is supported by 3D Printing Innovation Cell from Research and Development of Mr.R BUSINESS CORPORATION, Karur and Namakkal Branches, Tamilnadu India. We would like to express our gratitude to Er.N.Rajeswari CEO of the Mr.R BUSINESS CORPORATION.

Conflict of interest

The authors declare no conflict of interest.

References

1. Marino SG, Košťáková EK, Czél G. Development of pseudo-ductile interlayer hybrid composites of standard thickness plies by interleaving polyamide 6 nanofibrous layers. *Composites Science and Technology*. 2023, 234: 109924. doi: 10.1016/j.compscitech.2023.109924
2. Birosz MT, Safranyik F, Andó M. Concurrent shape and build orientation optimization for FDM additive manufacturing using the principal stress lines (PSL). *Heliyon*. 2023, 9(4): e15022. doi: 10.1016/j.heliyon.2023.e15022
3. Adapa SK, Jagadish. Prospects of Natural Fiber-Reinforced Polymer Composites for Additive Manufacturing Applications: A Review. *JOM*. 2023, 75(3): 920-940. doi: 10.1007/s11837-022-05670-w
4. Rajeshkumar G, Hariharan V, Indran S, et al. Influence of Sodium Hydroxide (NaOH) Treatment on Mechanical Properties and Morphological Behaviour of Phoenix sp. Fiber/Epoxy Composites. *Journal of Polymers and the Environment*. 2020, 29(3): 765-774. doi: 10.1007/s10924-020-01921-6
5. Baechle-Clayton M, Loos E, Taheri M, et al. Failures and Flaws in Fused Deposition Modeling (FDM) Additively Manufactured Polymers and Composites. *Journal of Composites Science*. 2022, 6(7): 202. doi: 10.3390/jcs6070202
6. Buj-Corral I, Zayas-Figuera EE. Comparative study about dimensional accuracy and form errors of FFF printed spur gears using PLA and Nylon. *Polymer Testing*. 2023, 117: 107862. doi: 10.1016/j.polymertesting.2022.107862
7. Sharma MP, Gupta PK, Kumar G. Process Parameters and Their Effect During Electrochemical Discharge Machining: A Review. *Emerging Trends in Mechanical and Industrial Engineering*. Published online 2023: 553-570. doi: 10.1007/978-981-19-6945-4_42
8. S., R., & A., J. R. (2023). Selection of polymer extrusion parameters by factorial experimental design—A decision making model. *Scientia Iranica*. doi: 10.24200/sci.2023.60096.6591
9. Abeykoon C, Sri-Amphorn P, Fernando A. Optimization of fused deposition modeling parameters for improved PLA and ABS 3D printed structures. *International Journal of Lightweight Materials and Manufacture*. 2020, 3(3): 284-297. doi: 10.1016/j.ijlmm.2020.03.003
10. Alhazmi MW, Backar A, Backar AH. Influence of infill density and orientation on the mechanical response of PLA+ specimens produced using FDM 3D printing fatigue behavior of austempered ductile iron view project

- stainless steels view project influence of infill density and orientation on. *Int. J. Adv. Sci. Technol*, 2020. 29(6): 3362–3371.
11. Banerjee D, Mishra SB, Sadique Khan M, et al. Mathematical approach for the geometrical deformation of fused deposition modelling build parts. *Materials Today: Proceedings*. 2020, 33: 5051-5054. doi: 10.1016/j.matpr.2020.02.842
 12. Ayatollahi MR, Nabavi-Kivi A, Bahrami B, et al. The influence of in-plane raster angle on tensile and fracture strengths of 3D-printed PLA specimens. *Engineering Fracture Mechanics*. 2020, 237: 107225. doi: 10.1016/j.engfracmech.2020.107225
 13. Deshwal S, Kumar A, Chhabra D. Exercising hybrid statistical tools GA-RSM, GA-ANN and GA-ANFIS to optimize FDM process parameters for tensile strength improvement. *CIRP Journal of Manufacturing Science and Technology*. 2020, 31: 189-199. doi: 10.1016/j.cirpj.2020.05.009
 14. Dave HK, Prajapati AR, Rajpurohit SR, et al. Investigation on tensile strength and failure modes of FDM printed part using in-house fabricated PLA filament. *Advances in Materials and Processing Technologies*. 2020, 8(1): 576-597. doi: 10.1080/2374068x.2020.1829951
 15. Farayibi PK, Omiyale BO. Mechanical Behaviour of Polylactic Acid Parts Fabricated via Material Extrusion Process: A Taguchi-Grey Relational Analysis Approach. *International Journal of Engineering Research in Africa*. 2020, 46: 32-44. doi: 10.4028/www.scientific.net/jera.46.32
 16. Kamaal M, Anas M, Rastogi H, et al. Effect of FDM process parameters on mechanical properties of 3D-printed carbon fibre–PLA composite. *Progress in Additive Manufacturing*. 2020, 6(1): 63-69. doi: 10.1007/s40964-020-00145-3
 17. Son TA, Minh PS, Thanh TD. Effect of 3D Printing Parameters on the Tensile Strength of Products. *Key Engineering Materials*. 2020, 863: 103-108. doi: 10.4028/www.scientific.net/kem.863.103
 18. Andreczyk A, Bagiński P, Klonowicz P. Numerical and experimental investigations of a turbocharger with a compressor wheel made of additively manufactured plastic. *International Journal of Mechanical Sciences*. 2020, 178: 105613. doi: 10.1016/j.ijmecsci.2020.105613
 19. Jiang S, Luo C, Lu Y. Multilayered nature in crystallization of polymer droplets studied by MD simulations: Orientation and entanglement. *Polymer*. 2023, 268: 125696. doi: 10.1016/j.polymer.2023.125696
 20. Ren G, Wan K, Kong H, et al. Recent advance in biomass membranes: Fabrication, functional regulation, and antimicrobial applications. *Carbohydrate Polymers*. 2023, 305: 120537. doi: 10.1016/j.carbpol.2023.120537
 21. Prieto C, Lagaron JM. Nanodroplets of Docosahexaenoic Acid-Enriched Algae Oil Encapsulated within Microparticles of Hydrocolloids by Emulsion Electrospraying Assisted by Pressurized Gas. *Nanomaterials*. 2020, 10(2): 270. doi: 10.3390/nano10020270
 22. Andrés MS, Chércoles R, Navarro E, et al. Use of 3D printing PLA and ABS materials for fine art. Analysis of composition and long-term behaviour of raw filament and printed parts. *Journal of Cultural Heritage*. 2023, 59: 181-189. doi: 10.1016/j.culher.2022.12.005
 23. Raja S, Agrawal AP, Patil P, et al. Optimization of 3D Printing Process Parameters of Polylactic Acid Filament Based on the Mechanical Test. Balaji GL, ed. *International Journal of Chemical Engineering*. 2022, 2022: 1-7. doi: 10.1155/2022/5830869
 24. Joseph TM, Kallingal A, Suresh AM, et al. 3D printing of polylactic acid: recent advances and opportunities. *The International Journal of Advanced Manufacturing Technology*. 2023, 125(3-4): 1015-1035. doi: 10.1007/s00170-022-10795-y
 25. Pulipaka A, Gide KM, Beheshti A, et al. Effect of 3D printing process parameters on surface and mechanical properties of FFF-printed PEEK. *Journal of Manufacturing Processes*. 2023, 85: 368-386. doi: 10.1016/j.jmapro.2022.11.057
 26. French AD, Anguiano SA, Bliss M, et al. Mass spectrometric investigations into 3D printed parts to assess radiopurity as ultralow background materials for rare event physics detectors. *Nuclear Instruments and Methods in Physics Research Section A: Accelerators, Spectrometers, Detectors and Associated Equipment*. 2023, 1047: 167830. doi: 10.1016/j.nima.2022.167830
 27. Hernandez-Carrillo I, Wood CJ, Liu H. Advanced materials for the impeller in an ORC radial microturbine. *Energy Procedia*. 2017, 129: 1047-1054. doi: 10.1016/j.egypro.2017.09.241
 28. Pavlovic A, Slijivic M, Krajsnik M, et al. Polymers in additive manufacturing: The case of a water pump impeller. *FME Transaction*. 2017, 45(3): 354-359. doi: 10.5937/fmet1703354p
 29. Polák M. Behaviour of 3D printed impellers in performance tests of hydrodynamic pump. In *Proceedings of the 7th International Conference on Trends in Agricultural Engineering, Prague, Czech Republic. 17–20 September 2019*; pp. 17–20.
 30. Kzyrov U, Turgali D. Performance Enhancement of a Centrifugal Pump by Impeller Retrofitting; Nazarbayev University School of Engineering and Digital Sciences: 2019. Available online: <https://nur.nu.edu.kz/bitstream/handle/123456789/4476/Performance%20Enhancement%20of%20a%20Centrifugal%20Pump%20by%20Impeller%20Retrofitting.pdf;jsessionid=3A3B30B32BD593170B53A63F8FFC63C9?sequence=5> (accessed on 7 July 2019).
 31. Kopparapu R, Mathew S, Siciliano E, et al. Designing a Centrifugal Pump System for High Altitude Water Crises. 2017.

32. Warner J, Celli D, Scott-Emuakpor O, et al. Fused Deposition Modeling Fabrication Evaluation of a Ti-6Al-4V Centrifugal Compressor. *Journal of Engineering for Gas Turbines and Power*. 2022, 145(3). doi: 10.1115/1.4055582
33. Matos T, Pinto V, Sousa P, et al. Design and In Situ Validation of Low-Cost and Easy to Apply Anti-Biofouling Techniques for Oceanographic Continuous Monitoring with Optical Instruments. *Sensors*. 2023, 23(2): 605. doi: 10.3390/s23020605
34. Mishra V, Negi S, Kar S. FDM-based additive manufacturing of recycled thermoplastics and associated composites. *Journal of Material Cycles and Waste Management*. 2023, 25(2): 758-784. doi: 10.1007/s10163-022-01588-2
35. Birosz MT, Andó M, Jeganmohan S. Finite Element Method modeling of Additive Manufactured Compressor Wheel. *Journal of The Institution of Engineers (India): Series D*. 2021, 102(1): 79-85. doi: 10.1007/s40033-021-00251-8
36. Yost S. Increased Interlayer Adhesion of Additively Manufactured Parts. 2023.
37. Hannouch A, Habchi C, Metni N, et al. Thermal analysis of a 3D printed thermal manikin inside an infant incubator. *International Journal of Thermal Sciences*. 2023, 183: 107826. doi: 10.1016/j.ijthermalsci.2022.107826
38. Subramani R, Kaliappan S, Sekar S, et al. Polymer Filament Process Parameter Optimization with Mechanical Test and Morphology Analysis. Thanigaivelan R, ed. *Advances in Materials Science and Engineering*. 2022, 2022: 1-8. doi: 10.1155/2022/8259804
39. Odetti A, Altosole M, Bruzzone G, et al. Design and Construction of a Modular Pump-Jet Thruster for Autonomous Surface Vehicle Operations in Extremely Shallow Water. *Journal of Marine Science and Engineering*. 2019, 7(7): 222. doi: 10.3390/jmse7070222.
40. Zywica G, Kaczmarczyk TZ, Ihnatowicz E, et al. Application OF a heat resistant plastic IN a high-speed microturbine designed for the domestic ORC system. *Int. Semin. ORC Power Syst.*, 2019. 1–8.
41. Malaga A, Vinodh S. Technology Selection for Additive Manufacturing in Industry 4.0 Scenario Using Hybrid MCDM Approach. *Industry 40 and Advanced Manufacturing*. Published online July 24, 2022: 207-217. doi: 10.1007/978-981-19-0561-2_19
42. Raja S, Rajan AJ. A Decision-Making Model for Selection of the Suitable FDM Machine Using Fuzzy TOPSIS. Gupta P, ed. *Mathematical Problems in Engineering*. 2022, 2022: 1-15. doi: 10.1155/2022/7653292
43. Ghuge S, Parhi S. Additive Manufacturing Service Provider Selection Using a Neutrosophic Best Worst Method. *Procedia Computer Science*. 2023, 217: 1550-1559. doi: 10.1016/j.procs.2022.12.355
44. Chandra M, Shahab F, KEK V, et al. Selection for additive manufacturing using hybrid MCDM technique considering sustainable concepts. *Rapid Prototyping Journal*. 2022, 28(7): 1297-1311. doi: 10.1108/rpj-06-2021-0155
45. Raja S, John Rajan A, Praveen Kumar V, et al. Selection of Additive Manufacturing Machine Using Analytical Hierarchy Process. Gupta P, ed. *Scientific Programming*. 2022, 2022: 1-20. doi: 10.1155/2022/1596590
46. Subramani R, Kaliappan S, Arul kumar PV, et al. A Recent Trend on Additive Manufacturing Sustainability with Supply Chain Management Concept, Multicriteria Decision Making Techniques. Thanigaivelan R, ed. *Advances in Materials Science and Engineering*. 2022, 2022: 1-12. doi: 10.1155/2022/9151839
47. Aydoğdu E, Güner E, Aldemir B, et al. Complex spherical fuzzy TOPSIS based on entropy. *Expert Systems with Applications*. 2023, 215: 119331. doi: 10.1016/j.eswa.2022.119331
48. Olaiya NG, Maraveas C, Salem MA, et al. Viscoelastic and Properties of Amphiphilic Chitin in Plasticised Polylactic Acid/Starch Biocomposite. *Polymers*. 2022, 14(11): 2268. doi: 10.3390/polym14112268
49. Sekhar KC, Surakasi R, Roy DrP, et al. Mechanical Behavior of Aluminum and Graphene Nanopowder-Based Composites. Balaji GL, ed. *International Journal of Chemical Engineering*. 2022, 2022: 1-13. doi: 10.1155/2022/2224482
50. Velmurugan G, Siva Shankar V, Kaliappan S, et al. Effect of Aluminium Tetrahydrate Nanofiller Addition on the Mechanical and Thermal Behaviour of Luffa Fibre-Based Polyester Composites under Cryogenic Environment. Lakshmipathy R, ed. *Journal of Nanomaterials*. 2022, 2022: 1-10. doi: 10.1155/2022/5970534
51. Karthick M, Meikandan M, Kaliappan S, et al. Experimental Investigation on Mechanical Properties of Glass Fiber Hybridized Natural Fiber Reinforced Penta-Layered Hybrid Polymer Composite. Balaji GL, ed. *International Journal of Chemical Engineering*. 2022, 2022: 1-9. doi: 10.1155/2022/1864446
52. Natrayan L, Kaliappan S, Baskara Sethupathy S, et al. Investigation on Interlaminar Shear Strength and Moisture Absorption Properties of Soybean Oil Reinforced with Aluminium Trihydrate-Filled Polyester-Based Nanocomposites. R L, ed. *Journal of Nanomaterials*. 2022, 2022: 1-8. doi: 10.1155/2022/7588699
53. Tamil Mannan K, Sivaprakash V, Raja S, et al. Effect of Roselle and biochar reinforced natural fiber composites for construction applications in cryogenic environment. *Materials Today: Proceedings*. 2022, 69: 1361-1368. doi: 10.1016/j.matpr.2022.09.003
54. Velu R, Tulasi R, Ramachandran MK. Environmental Impact, Challenges for Industrial Applications and Future Perspectives of Additive Manufacturing. *Nanotechnology-Based Additive Manufacturing*. Published online December 23, 2022: 691-709. doi: 10.1002/9783527835478.ch24

55. Tamil Mannan K, Sivaprakash V, Raja S, et al. Significance of Si₃N₄/Lime powder addition on the mechanical properties of natural calotropis gigantea composites. *Materials Today: Proceedings*. 2022, 69: 1355-1360. doi: 10.1016/j.matpr.2022.09.002
56. He F, Yuan L, Mu H, et al. Research and application of artificial intelligence techniques for wire arc additive manufacturing: a state-of-the-art review. *Robotics and Computer-Integrated Manufacturing*. 2023, 82: 102525. doi: 10.1016/j.rcim.2023.102525
57. Guo H, Xu J, Zhang S, et al. Multi-orientation optimization of complex parts based on model segmentation in additive manufacturing. *Journal of Mechanical Science and Technology*. 2023, 37(1): 317-331. doi: 10.1007/s12206-022-1231-2
58. Li S, Johnson MS, Sitnikova E, et al. Laminated beams/shafts of annular cross-section subject to combined loading. *Thin-Walled Structures*. 2023, 182: 110153. doi: 10.1016/j.tws.2022.110153
59. Raja S, Logeshwaran J, Venkatasubramanian S, et al. OCHSA: Designing Energy-Efficient Lifetime-Aware Leisure Degree Adaptive Routing Protocol with Optimal Cluster Head Selection for 5G Communication Network Disaster Management. Gupta P, ed. *Scientific Programming*. 2022, 2022: 1-11. doi: 10.1155/2022/5424356
60. Heinisuo M, Pajunen S, Aspila A. Ultimate failure load analysis of cross-laminated timber panels subjected to in-plane compression. *Structures*. 2023, 47: 1558-1565. doi: 10.1016/j.istruc.2022.12.016
61. Raja S, Logeshwaran J, Venkatasubramanian S, et al. OCHSA: Designing Energy-Efficient Lifetime-Aware Leisure Degree Adaptive Routing Protocol with Optimal Cluster Head Selection for 5G Communication Network Disaster Management. Gupta P, ed. *Scientific Programming*. 2022, 2022: 1-11. doi: 10.1155/2022/5424356
62. Ji C, Hu J, Sadighi M, et al. Experimental and theoretical study on residual ultimate strength after impact of CF/PEEK-titanium hybrid laminates with nano-interfacial enhancement. *Composites Science and Technology*. 2023, 232: 109871. doi: 10.1016/j.compscitech.2022.109871
63. Kmita-Fudalej G, Szewczyk W, Kołakowski Z. Bending Stiffness of Honeycomb Paperboard. *Materials*. 2022, 16(1): 156. doi: 10.3390/ma16010156
64. Kam M, Saruhan H, İpekçi A. Investigation the Effect of 3d Printer System Vibrations on Surface Roughness of the Printed Products. *Düzce Üniversitesi Bilim ve Teknoloji Dergisi*. 2019, 7(2): 147-157. doi: 10.29130/dubited.441221
65. Srinivasan R, Pridhar T, Ramprasath LS, et al. Prediction of tensile strength in FDM printed ABS parts using response surface methodology (RSM). *Materials Today: Proceedings*. 2020, 27: 1827-1832. doi: 10.1016/j.matpr.2020.03.788
66. Dev S, Srivastava R. Experimental investigation and optimization of FDM process parameters for material and mechanical strength. *Materials Today: Proceedings*. 2020, 26: 1995-1999. doi: 10.1016/j.matpr.2020.02.435
67. Radhwan H, Shayfull Z, Abdellah AEH, et al. Optimization parameter effects on the strength of 3D-printing process using Taguchi method. *AIP Conference Proceedings*. Published online 2019. doi: 10.1063/1.5118162
68. Garzon-Hernandez S, Garcia-Gonzalez D, Jérusalem A, et al. Design of FDM 3D printed polymers: An experimental-modelling methodology for the prediction of mechanical properties. *Materials & Design*. 2020, 188: 108414. doi: 10.1016/j.matdes.2019.108414
69. Kiendl J, Gao C. Controlling toughness and strength of FDM 3D-printed PLA components through the raster layup. *Composites Part B: Engineering*. 2020, 180: 107562. doi: 10.1016/j.compositesb.2019.107562
70. Praveenkumar V, Raja S, Jamadon NH, et al. Role of laser power and scan speed combination on the surface quality of additive manufactured nickel-based superalloy. *Proceedings of the Institution of Mechanical Engineers, Part L: Journal of Materials: Design and Applications*. Published online November 13, 2023. doi: 10.1177/14644207231212566
71. Alafaghani A, Qattawi A, Alrawi B, et al. Experimental Optimization of Fused Deposition Modelling Processing Parameters: A Design-for-Manufacturing Approach. *Procedia Manufacturing*. 2017, 10: 791-803. doi: 10.1016/j.promfg.2017.07.079
72. Huu NH, Phuoc DP, Huu TN, et al. Optimization of The FDM Parameters to Improve The Compressive Strength of The PLA-copper Based Products. *IOP Conference Series: Materials Science and Engineering*. 2019, 530(1): 012001. doi: 10.1088/1757-899x/530/1/012001